

**UV-INDUCED LUMINESCENCE PROPERTIES OF SrAl<sub>2</sub>O<sub>4</sub>: Eu<sup>2+</sup>, Dy<sup>3+</sup> NANOPHOSPHORS****D.S. KSHATRI<sup>a1</sup>, SHUBHRA MISHRA<sup>b</sup>, AYUSH KHARE<sup>c</sup> AND ANGESH CHANDRA<sup>d</sup>**<sup>abd</sup>Department of Physics, Shri Shankaracharya Institute of Professional Management and Technology, Raipur, India<sup>c</sup>Department of Physics, National Institute of Technology, Raipur, India**ABSTRACT**

A low temperature combustion synthesis technique (CST) is used to synthesize the SrAl<sub>2</sub>O<sub>4</sub>: Eu<sup>2+</sup>, Dy<sup>3+</sup> nanophosphor. X-ray diffraction (XRD), field emission scanning electron microscopy (SEM), high resolution transmission electron microscopy (HRTEM) and energy dispersive X-ray spectroscopy (EDX) are used to examine the surface morphology and structural properties of as-synthesized nanophosphor. The optical properties are discussed in terms of photoluminescence (PL) and afterglow decay spectra. To study the effects of ultraviolet (UV) light, as-obtained SrAl<sub>2</sub>O<sub>4</sub>: Eu<sup>2+</sup>, Dy<sup>3+</sup> phosphor is then exposed with UV light 5, 10, 15, 20 and 25 min. and observed that higher PL emission intensity is recorded at 515 nm (green emission) for 25 min. UV-induced nanophosphor. After being irradiated with UV light for maximum time (25 min.), the phosphor emits green long lasting phosphorescence (LLP) suggesting potential applications in many fields.

**KEYWORDS:** XRD, HRTEM, Photoluminescence, Afterglow

The researchers have focused on divalent europium (Eu<sup>2+</sup>) as the activating ion after the discovery of SrAl<sub>2</sub>O<sub>4</sub>: Eu<sup>2+</sup>, Dy<sup>3+</sup> in 1996 [Matsuzawa et. al.]. The synthesis of these materials for display applications with considerably good initial brightness and long afterglow has been a major goal of many research groups [Jia et. al., 2001]. Commercially available microcrystalline SrAl<sub>2</sub>O<sub>4</sub> phosphors are usually prepared by a solid-state reaction technique (SSRT) [Kshatri and Khare, 2014] and smaller particles in nano-range are obtained by combustion synthesis technique (CST) [Kshatri and Khare, 2014]. The Combustion synthesis technique (CST) or self-propagating high-temperature synthesis (SHS), on the other hand is an effective, low-cost method for producing various industrially useful nanocrystalline materials. The combustion process to prepare powder samples, however, is very facile and only takes few minutes, which has been extensively applied to the preparation of various nano sized oxide materials. The SrAl<sub>2</sub>O<sub>4</sub>: Eu<sup>2+</sup>, Dy<sup>3+</sup> phosphor resulted from CST has optical properties similar to phosphor resulted from the former method but the sintering temperature of the sample is much lower than that prepared by solid state reaction or sol-gel method. Shafia et al., 2010 reported the spectroscopic and host phase properties of SrAl<sub>2</sub>O<sub>4</sub>: Eu<sup>2+</sup>, Dy<sup>3+</sup> phosphors with a series of different initiating combustion temperature, urea concentration as a fuel and critical pH of precursor solution. The SrAl<sub>2</sub>O<sub>4</sub>: Eu<sup>2+</sup>, Dy<sup>3+</sup> nanoparticle pigments were obtained by exothermic combustion process within less than 5 min. Recently, a number of important breakthroughs in this field have been made, notably for development of new catalysts and nano carriers with properties better than those for similar traditional materials [Patil et. al., 2002].

Combustion synthesis route gives a fluffy mass reducible to quite fine particles with almost no effort. Conditions prevailing during the processing should favor formation of fine particles in sub-micron region. Oxidizing atmosphere prevails in combustion process [Katsumata et. al., 1998]. Incorporation of europium in bivalent state invariably requires reducing atmosphere [Shanker et. al., 2000]. With a view to develop a process for the instant synthesis of nano phase particles of the phosphor, we employed combustion route [Suriyamurthy and Panigrahi, 2008].

In the present paper, we present and discuss the results of synthesis, characterization and optical studies of most intense nanocrystalline Sr<sub>0.97</sub>Al<sub>2</sub>O<sub>4</sub>: Eu<sup>2+</sup><sub>0.01</sub>, Dy<sup>3+</sup><sub>0.02</sub> phosphor [Kshatri and Khare, 2014] prepared by combustion synthesis techniques.

**EXPERIMENTAL****Materials and Method**

In order to prepare microcrystalline Sr<sub>0.97</sub>Al<sub>2</sub>O<sub>4</sub>: Eu<sup>2+</sup><sub>0.01</sub>, Dy<sup>3+</sup><sub>0.02</sub> phosphor, SrCO<sub>3</sub>, Al<sub>2</sub>O<sub>3</sub>, Eu<sub>2</sub>O<sub>3</sub> and Dy<sub>2</sub>O<sub>3</sub> (all 99.99 pure, supplied by Merck) are taken as starting materials and appropriate amount of boric acid (H<sub>3</sub>BO<sub>3</sub>) is also used as flux.

Nanocrystalline Sr<sub>0.97</sub>Al<sub>2</sub>O<sub>4</sub>: Eu<sup>2+</sup><sub>0.01</sub>, Dy<sup>3+</sup><sub>0.02</sub> powder phosphor is synthesized using Sr(NO<sub>3</sub>)<sub>2</sub>, Al(NO<sub>3</sub>)<sub>3</sub>·9H<sub>2</sub>O, Eu<sub>2</sub>O<sub>3</sub>, Dy<sub>2</sub>O<sub>3</sub> (all 99.99 pure, supplied by Merck), urea [CO (NH<sub>2</sub>)<sub>2</sub>, AR] and boric acid (H<sub>3</sub>BO<sub>3</sub>, AR). For preparing NC samples, the crucible comprising of mixture of above compounds was placed into a furnace already maintained at a temperature of 600±5°C. The

preparational method is discussed in detail previously [Kshatri and Khare, 2014].

### Characterization Techniques

A Bruker Advance D8 X-ray diffractometer was used to get the powder XRD profiles of as-synthesized phosphors. The morphology of particles was examined using a ZEISS-EVO 60m German make scanning electron microscope (SEM). The crystallographic analysis and size determination of the phosphors were carried out by HRTEM and SAED using Model JEM 2100. Energy dispersive X-ray (EDX) spectroscopy was carried out with Oxford Inca EDX System. The excitation and emission spectra were recorded using Hitachi fluorescence spectrophotometer (Model: F-2500). The afterglow measurements were made with an indigenous experimental set-up comprising of a photomultiplier tube (RCA-931) and a digital nanoammeter (Model: DNM-121).

## RESULTS AND DISCUSSION

### XRD Analysis

The monoclinic phase of as-prepared nanocrystalline Sr<sub>0.97</sub>Al<sub>2</sub>O<sub>4</sub>: Eu<sup>2+</sup><sub>0.01</sub>, Dy<sup>3+</sup><sub>0.02</sub> phosphor was confirmed by the powder X-ray diffraction as shown in Figure 1. The patterns were indexed to the JCPDS card no 34-0379. Various diffraction peaks for nanocrystalline SrAl<sub>2</sub>O<sub>4</sub> phosphors are observed for 2θ = 23°, 33°, 34°, 35°, 41° and 48° corresponding to the planes (020), (-211), (220), (211), (031) and (040) respectively. All these peaks signify the presence of α-phase monoclinic SrAl<sub>2</sub>O<sub>4</sub> [Kshatri and Khare, 2014].

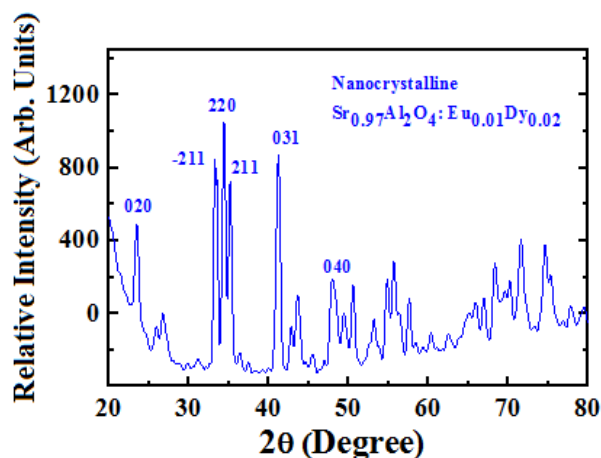


Figure 1: X-ray diffractogram of nanocrystalline Sr<sub>0.97</sub>Al<sub>2</sub>O<sub>4</sub>: Eu<sup>2+</sup><sub>0.01</sub>Dy<sup>3+</sup><sub>0.02</sub> phosphor

### SEM Analysis

Figure 2 shows the SEM micrograph nanocrystalline Sr<sub>0.97</sub>Al<sub>2</sub>O<sub>4</sub>: Eu<sup>2+</sup><sub>0.01</sub>, Dy<sup>3+</sup><sub>0.02</sub> phosphor. The combustible ash and fluffy form and comparatively smaller particles are observed in nanophosphor sample. Agglomeration in particles is witnessed. The sample possesses irregular morphology with angularity and corners. The surfaces of the foams show a lot of cracks, voids and pores created by the gases escaping during combustion reaction. Actually in CST large amount of escaping gases dissipate heat and thereby forbids the material from sintering and thus supports the formation of nano phase. However, the large surface area has the serious drawback that it may introduce various defects causing non-radiative recombination routes for electrons and holes and thus resulting in the lowering of luminescent intensity [Cheng et al., 2014].

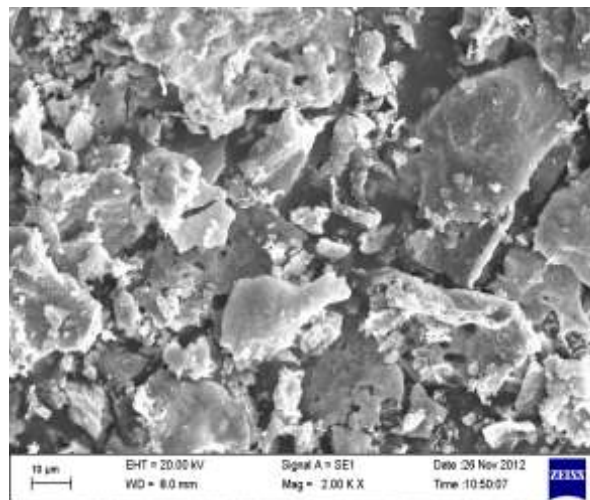
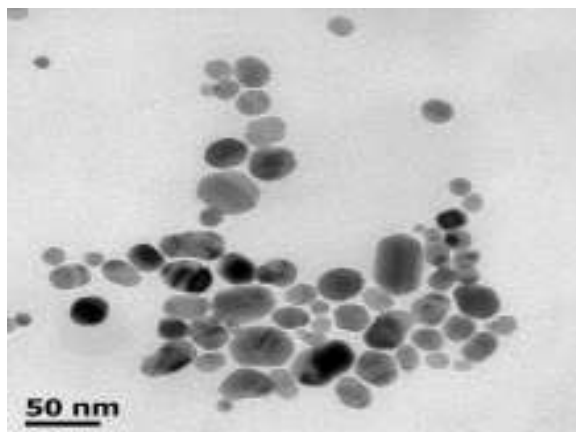


Figure 2: SEM micrograph nanocrystalline Sr<sub>0.97</sub>Al<sub>2</sub>O<sub>4</sub>: Eu<sup>2+</sup><sub>0.01</sub>Dy<sup>3+</sup><sub>0.02</sub> phosphor

### HRTEM Analysis

The HRTEM microstructure nanocrystalline Sr<sub>0.97</sub>Al<sub>2</sub>O<sub>4</sub>: Eu<sup>2+</sup><sub>0.01</sub>, Dy<sup>3+</sup><sub>0.02</sub> phosphor is depicted in figure 3. It is clearly observed phosphor is spherical in shape and having uneven surface and is highly agglomerated, which confirms that dopant and co-dopant ions are densely diffused into the SrAl<sub>2</sub>O<sub>4</sub> host lattice. The average diameters of nanophosphors are found to be approximately 25 nm, which strongly support the formation of nano particles and are consistent with the crystallite size estimated from XRD data. The HRTEM images illustrate the narrow size distribution in nano phosphor.



**Figure 3: HRTEM micrograph nanocrystalline Sr<sub>0.97</sub>Al<sub>2</sub>O<sub>4</sub>: Eu<sup>2+</sup><sub>0.01</sub>Dy<sup>3+</sup><sub>0.02</sub> phosphor**

#### EDX Analysis

The EDX profile of nanocrystalline Sr<sub>0.97</sub>Al<sub>2</sub>O<sub>4</sub>: Eu<sup>2+</sup><sub>0.01</sub>, Dy<sup>3+</sup><sub>0.02</sub> phosphor is depicted in figure 4. This measurement confirms the presence of constituents Al, Sr, O, Eu and Dy in the powder phosphor. No compositional variation is witnessed upon probing different locations within each powder sample indicating that they are homogenous. On the basis of calculations made for Sr<sub>0.97</sub>Al<sub>2</sub>O<sub>4</sub>: Eu<sub>0.01</sub> Dy<sub>0.02</sub> phosphor, the ratio of Sr: Al: O: Eu: Dy is 11.74: 21.23: 64.32: 0.57: 2.14 indicating that Eu<sup>2+</sup> with Dy<sup>3+</sup> ions are completely doped into SrAl<sub>2</sub>O<sub>4</sub> host matrix [Kshatri and Khare, 2014].

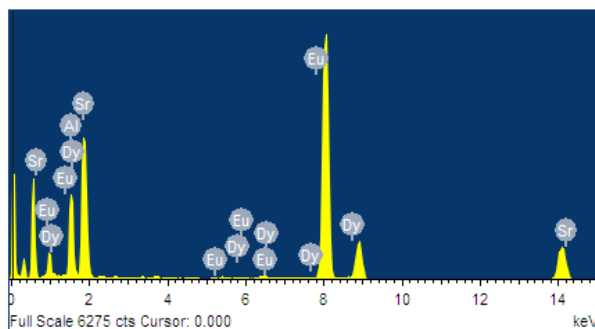


**Figure 4: EDX spectrum of nanocrystalline Sr<sub>0.97</sub>Al<sub>2</sub>O<sub>4</sub>: Eu<sup>2+</sup><sub>0.01</sub>Dy<sup>3+</sup><sub>0.02</sub> phosphor**

#### Photoluminescence Studies

Figure 5 shows the excitation spectrum and emission spectra of Sr<sub>0.97</sub>Al<sub>2</sub>O<sub>4</sub>: Eu<sub>0.01</sub> Dy<sub>0.02</sub> phosphor sample at different times (5, 10, 15, 20 and 25 minutes) of exposure of UV light ( $\lambda=365$  nm). The large bandwidths of the observed peaks are attributed to transitions between the 4f<sup>6</sup>5d<sup>1</sup> and 4f<sup>7</sup> electron of Eu<sup>2+</sup> [Xu et. al., 2008]. The excitation spectra indicate the possibility of SrAl<sub>2</sub>O<sub>4</sub>: Eu<sup>2+</sup>,

Dy<sup>3+</sup> being excited by a broad range of light including visible light. It displays the intensity and the wavelength of the emission when the phosphor is excited by UV light ( $\lambda=365$  nm) for different times. It is observed that the maximum emission intensity is exhibited for longest time (25 min.) and minimum is for shortest time (5 min.) at around 515 nm, which is in good agreement with afterglow characteristics of Sr<sub>0.97</sub>Al<sub>2</sub>O<sub>4</sub>: Eu<sub>0.01</sub> Dy<sub>0.02</sub> phosphor as discussed further. It is important to recall that the persistent luminescence is mainly due to the slow radiative recombination of trapped charges after they are thermally released into the conduction (electrons) or valence (holes) band [Kshatri and Khare, 2014].

The broad emission band peaking is attributed to the typical 4f<sup>6</sup>5d<sup>1</sup>-4f<sup>7</sup> transitions of Eu<sup>2+</sup>, where the lowest excited state of 4f levels of Eu<sup>2+</sup> is located higher than the 4f<sup>6</sup>5d<sup>1</sup> level in most crystals, so that Eu<sup>2+</sup> usually gives broad-band emission due to f-d transitions [Yamamoto and Matsuzawa, 1997; Haranath et. al., 2003 & Meng et. al., 2005].

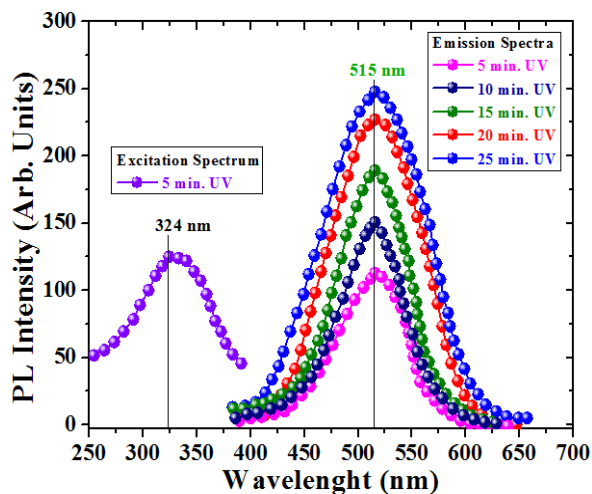


**Figure 5: Excitation spectrum and Emission spectra of Sr<sub>0.97</sub>Al<sub>2</sub>O<sub>4</sub>: Eu<sub>0.01</sub> Dy<sub>0.02</sub> phosphor at different times of exposure of UV light ( $\lambda=365$  nm)**

#### Afterglow Characteristics

Figure 6 presents the luminescent decay curves of Sr<sub>0.97</sub>Al<sub>2</sub>O<sub>4</sub>: Eu<sub>0.01</sub> Dy<sub>0.02</sub> phosphor irradiated by UV light ( $\lambda=365$ nm) for different times. From figure, it is clear that all the afterglow decay curves are composed of three regimes; the fast, intermediate and the subsequent slow-decaying process. The fast-decaying process is due to the short survival time of electrons in Eu<sup>2+</sup> state while the slow-decaying process owes to the deep trap energy center

of Dy<sup>3+</sup> [Qiu et. al., 2007]. The Eu<sup>2+</sup> and Dy<sup>3+</sup> ions in aluminates phosphors are the luminescent centers and the traps respectively. The long afterglow property usually results from the trap energy level produced by doping of Eu<sup>2+</sup> and Dy<sup>3+</sup> ions in the crystals. In fact, SrAl<sub>2</sub>O<sub>4</sub>: Eu<sup>2+</sup>, Dy<sup>3+</sup> phosphor is monoclinic structure, which gives rise to the formation of appropriate trap for producing afterglow (Chen et al., 2001). It can be observed that decay time is being increased with UV-exposure time and it is maximum for 25 min. of UV-exposure [Kshatri and Khare, 2014].

The decay behavior can be analyzed by a curve fitting procedure relying on the following triple exponential equation [Dejene et. al., 2013]:

$$I = C_1 \exp\left(\frac{-t}{\tau_1}\right) + C_2 \exp\left(\frac{-t}{\tau_2}\right) + C_3 \exp\left(\frac{-t}{\tau_3}\right) \quad (1)$$

where I represents the phosphorescent intensity; C<sub>1</sub>, C<sub>2</sub> and C<sub>3</sub> are constants; t is the time and τ<sub>1</sub>, τ<sub>2</sub> and τ<sub>3</sub> are decay times for the fast, intermediate and slow exponential components respectively.

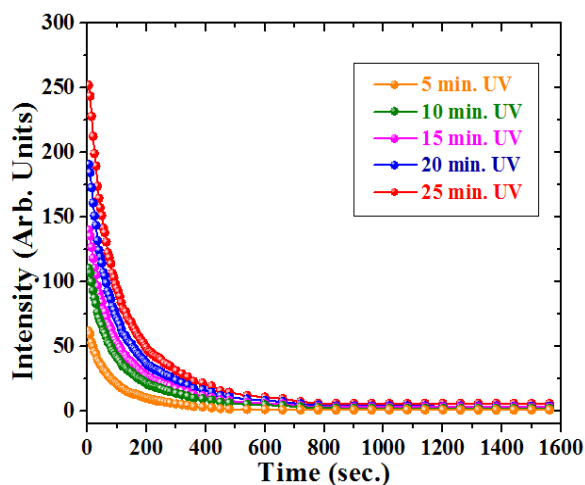


**Figure 6: Afterglow decay curves of Sr<sub>0.97</sub>Al<sub>2</sub>O<sub>4</sub>: Eu<sub>0.01</sub> Dy<sub>0.02</sub> phosphor at different times of exposure of UV light (λ=365 nm)**

## CONCLUSION

The nanocrystalline Sr<sub>0.97</sub>Al<sub>2</sub>O<sub>4</sub>: Eu<sub>0.01</sub> Dy<sub>0.02</sub> phosphor is synthesized successfully by CST. The results of XRD studies confirm the α-phase monoclinic structure of SrAl<sub>2</sub>O<sub>4</sub>. The FWHM supports the formation of nanophase

particles. The EDX results confirm the doping of Eu<sup>2+</sup> and Dy<sup>3+</sup> in the SrAl<sub>2</sub>O<sub>4</sub> host matrix. The HRTEM results show the formation of nanocrystalline phosphor. The PL and afterglow behavior show that maximum intensity and highest decay time is observed for the phosphor which is exposed to UV light for 25 min.

## REFERENCES

- Matsuzawa T., Aoki Y., Takeuchi N. and Murayama Y., 1996. *J. Electrochem. Soc.*, **143**: 2670.
- Jia D., Zhu J. and Wu B., 2001. *J. Lumin.*, **93**: 107.
- Kshatri D.S. and Khare A., 2014. *J. Lumin.*, **155**: 257.
- Shafia E., Bodaghi M. and Tahriri M., 2010. *Curr. Appl. Phys.*, **10**: 596.
- Patil K.C., Aruna S.T. and Mimani T., 2002. *Curr. Opin. Sol. Stat. Mat. Sci.*, **6**: 507.
- Katsumata T., Sasajima K., Nabae T., Komuro S. and Morikawa T., 1998. *J. Am. Ceram. Soc.*, **81**: 413.
- Shanker V., Chander H. and Ghosh P.K., 2000. *Proc. Intl. Symp. on Lumin. and its Appl.*, 96.
- Suriyamurthy N. and Panigrahi B. S., 2008. *J. Lumin.*, **128**:1809.
- Kshatri D.S. and Khare A., 2014. *J. Alloys and Comp.*, **588**:488.
- Cheng X., Lowe S.B. and Reece P.J., 2014. *J. J. Gooding, Chem. Soc. Rev.*, DOI: 10.1039/C3CS60353A (2014).
- Xu X., Caol L., Jiang D. and Li Q., 2008. *Key Engg. Mat.*, **381**: 368.
- Yamamoto H. and Matsuzawa T., 1997. *J. Lumin.*, **287**: 72–74.
- Haranath D., Shanker V., Chander H. and Sharma P., 2003. *J. Phys. D: Appl. Phys.*, **36**: 2244.
- Meng Y., Wang D., Li L. and Shi Z., 2005. *J. Chin. Rare Earth Soc.*, **23**: 277.
- Qiu Z., Zhou Y., Lu M., Zhang A. and Ma Q., 2007. *Acta Mater.*, **55**: 2615.
- Dejene F.B., Kebede M.A., Redi-Abshiro M. and Kgarebe B.V., 2013. *Opt. Mater.*, **35**:1927.